Arabian Journal of Chemistry (2014) 7, 425–435

King Saud University

Arabian Journal of Chemistry

www.ksu.edu.sa
www.sciencedirect.com

ORIGINAL ARTICLE

2nd Cancer Update

Theoretical investigation of inclusion complex formation of Gold (III) – Dimethyldithiocarbamate anticancer agents with cucurbit[*n* = 5,6]urils

Zabiollah Mahdavifar *, Sepideh Samiee

Computational Chemistry Group, Department of Chemistry, Faculty of Science, Shahid Chamran University, Ahvaz, Iran

Received 10 August 2012; accepted 9 February 2013
Available online 28 February 2013

KEYWORDS

Gold(III);
Dimethyldithiocarbamate;
Anticancer drugs;
Encapsulation;
Cucurbit[*n*]uril;
DFT calculation

Abstract Gold (III)-N,N-dimethyldithiocarbamate [DMDT(Au)X_2] complexes have recently gained increasing attention as potential anticancer agents because of their strong tumor cell growth–inhibitory effects, generally achieved by exploiting non-cisplatin-like mechanisms of action. The goal of our research work is to encapsulate the gold(III) dimethyldithiocarbamate complexes as anticancer with cucurbit[*n*]urils (CB[*n* = 5, 6]) by accurate calculations, to predict the inclusion complex formation of gold(III) species with cucurbiturils (CB[*n* = 5, 6]). The calculations were carried out just for the 1:1 stoichiometric complexes. Upon encapsulation, binding energy, thermodynamic parameters, structural parameters and electronic structures of complexes are investigated. The results of the thermodynamic calculations and the binding energy show that the inclusion process is exothermic and the CB[6]/[DMDT(Au)Br_2] complex is more stable than other complexes. The final geometry of CB[*n*]/drugs indicates that the drugs were expelled from the cavity of CB[*n*]. NBO calculations reveal that the hydrogen bonding between CB[*n*] and drugs and electrostatic interactions are the major factors contributing to the overall stabilities of the complexes.

1. Introduction

Since the introduction of Pt(II)-based first anticancer agents, metal complexes and organometallic compounds have been gaining growing importance in cancer therapy. The impressive clinical effectiveness of cisplatin is limited by significant side effects and by acquired or intrinsic resistance to the treatment (Kelland, 2007). Thus, classic and unconventional Pt(II) and Pt(IV) complexes have been introduced in therapy or are presently in advanced clinical trials. Moreover, innovative non-platinum metal-based antitumor agents, whose activity do

* Corresponding author. Tel.: +98 916 3015227; fax: +98 611 3331042.
E-mail addresses: zb_nojini@scu.ac.ir, zb.nojini@gmail.com (Z. Mahdavifar).
Peer review under responsibility of King Saud University.

Production and hosting by Elsevier

1878-5352 © 2013 King Saud University. Production and hosting by Elsevier B.V. All rights reserved.
http://dx.doi.org/10.1016/j.arabjc.2013.02.012

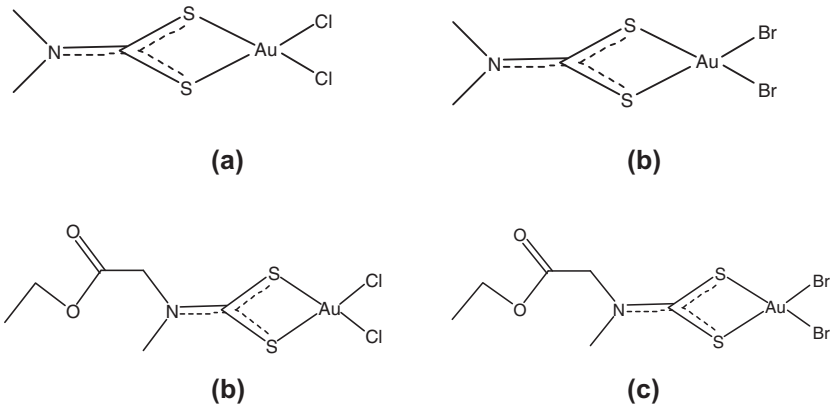

Figure 1 Gold(III) complexes with Au–S bonds (a) [DMDT(Au)Cl_2], (b) [DMDT(Au) Br_2], (c) [ESDT(Au)Cl_2] and (d) [ESDT(Au)Br_2].

not rely on direct DNA damage and may involve proteins and enzymes, have been developed (Alama1 et al., 2009). Of the non-platinum metal compounds with antitumor activity, particular interest has been focused on gold and tin derivatives, which have a common activity on mitochondria and a strong affinity to thiol groups of proteins and enzymes (Louie and Meade, 1999; Robertson and Orrenius, 2002).

Based on their structural and electronic similarity to cisplatin and cisplatin-related antitumor drugs gold(III) species represent a promising class of potential anticancer agents. However, the development of gold(III) complexes as therapeutic drugs has been hampered by their low stability under physiological conditions which remains a critical parameter in the drug development of these species. Gold(III) complexes with various ligands have been prepared and biologically investigated (Gabbiani et al., 2007; Marzano et al., 2011). Most of them are complexes with Au–N bonds (eventually containing additional Au–O and Au–Cl bonds) but also some species with Au–S or Au–C bonds and their bioactivities have been described (Ott, 2009). Gold(III) complexes (see Fig. 1 for some relevant examples) exhibited superior cytotoxic effects to cisplatin, being also active in resistant cells and induced apoptosis (Giovagnini et al., 2005; Ronconi et al., 2005). The compounds showed good stability under physiological conditions, bind readily to the DNA, inhibit both DNA and RNA synthesis and induce fast DNA lesions. Experiments on red blood cells indicated that hemolytic properties might contribute significantly to the bioactivity of the agents (Ronconi et al., 2006).

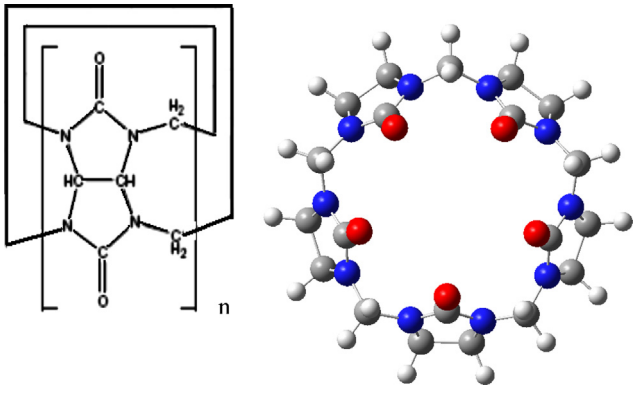

Figure 2 General structures of cucurbit[n]urils.

Cucurbit[*n*]urils (CB[*n*]), a family of pumpkin-like molecular containers, are cyclic methylene-bridged glycoluril oligomers with two portals lined by ureido carbonyl groups (Fig. 2) that provide entry to their hydrophobic cavity (Lei et al., 2010). While Cucurbit[6]uril (CB[6]) was first discovered in 1905 (Behrend et al., 1905) and its macrocyclic structure was not determined until 1981 in 2000, CB[6] was the one of the only cucurbit[*n*]uril to receive any attention as a molecule useful in the host–guest chemistry (Freeman et al., 1981). This changed upon the discovery of different sized cucurbit[*n*]urils: CB[5], CB[7], CB[8] and the isolation of free CB[10] (Kim et al., 2000; Liu et al., 2005). Their discovery has led to a rapid increase in the interest in the use of, CB[*n*] in a variety of fields including: nano machines, chromatography, and drug delivery (Wyman and Macartney, 2010).

There has been an increasing interest recently in using cyclodextrins and cucurbit[*n*]urils to aid in the delivery of molecules of biological and medicinal interest, through host–guest formation (Bali et al., 2006; Lagona et al., 2005; Faustino et al., 2011; Sancho et al., 2011). Cucurbit[*n*]urils can encapsulate a variety of molecules within their hydrophobic cavity, with the binding potentially further stabilized by favorable electrostatic and hydrogen bonding interactions with the carbonyl rimmed portals (Bali et al., 2006). Encapsulation of drugs inside a cucurbit[*n*]uril provides two benefits. Protects the drugs from degradation and increases the specificity of the drugs, and uptake into cancerous cells. Consequently, encapsulation in cucurbit[*n*]uril would protect the metal complexes such as platinum complex from reactions with plasma proteins in the bloodstream, but would not affect the reaction of the metal complex with DNA inside the cell (Bali et al., 2006). There has been increasing interest recently in using cucurbit[*n*]urils to aid in the delivery of molecules of biological and medicinal interest, through host–guest formation. Cucurbit[7]uril and cucurbit[8]uril molecules have been used to form host–guest complexes with mononuclear, dinuclear and trinuclear platinum(II) complexes (Wheate et al., 2004; Wheate, 2008; Wang and Macartney, 2008; Anconi et al., 2011). There are many reports on the theoretical studies of CB[*n*] (Marquez et al., 2004; Pichierri, 2006; Buschmann et al., 2006; Bakovets et al., 2008; Suvitha et al., 2010). Kim and coworkers have shown that the inclusion complex formation of oxaliplatin with cucurbit[7]uril has moderate cytotoxicity with a larger decrease in reactivity toward guanosine and L-methionine, respectively (Jeon et al., 2005). Gejji and coworkers, made an

assessment on the complex formation capability of CB[*n*] with ferrocene (Pinjari and Gejji, 2008).

Density functional theory has been successful in rationalizing popular concepts such as chemical reactivity and selectivity of molecules based on their global and local reactivity indices. The global index includes electronegativity (χ) (Sen and Jorgensen, 1987) and hardness (η) (Sen and Jorgensen, 1987; Pearson, 1997), while the local index includes the Fukui function ($f(r)$ and ($s(r)$) (Yang and Parr, 1985). As we already know, electronegativity may be considered as the power of an atom in a given molecule to attract electrons to itself (Parr and Yang, 1984). The idea of hardness was given by Pearson in the context of the hard–soft-acid–base (HSAB) (Pearson, 1973) principle, which states that "hard likes hard and soft likes soft". Another hardness-based principle is the maximum hardness principle (MHP) (Pearson, 1993), which states that "it seems to be a rule of nature that molecules arrange themselves so as to be as hard as possible" (Pearson, 1987). For a *N*-electron system with potential to act on an electron at **r** due to the nuclear attraction plus such other external forces as may be present external potential $\mathbf{v}(\mathbf{r})$ and total energy E, electronegativity (χ) (Sen and Jorgensen, 1987) and hardness (η) (Pearson, 1993) are defined as the following first-order (Pearson et al., 1978) and second-order (Parr and Pearson, 1983) derivatives, respectively:

$$\chi = -\left(\frac{\partial E}{\partial N}\right)_{v(\mathbf{r}),T} = -\mu \tag{1}$$

$$\eta = \frac{1}{2}\left(\frac{\partial^2 E}{\partial N^2}\right)_{v(\mathbf{r}),T} = \frac{1}{2}\left(\frac{\partial \mu}{\partial N}\right)_{v(\mathbf{r}),T} \tag{2}$$

where μ is the electronic chemical potential, defined as the negative of electronegativity. In addition, the global softness, S, of the equilibrium state of an electronic system at temperature T, is defined as (Parr and Yang, 1989):

$$S = \frac{1}{2\eta} = \left(\frac{\partial N}{\partial \mu}\right)_{v(\mathbf{r}),T} \tag{3}$$

Recently, Parr and co-workers (Pearson et al., 1999) have introduced an electrophilicity index (w), as:

$$w = \left(\frac{\mu^2}{2\eta}\right) \tag{4}$$

It was proposed as a measure of the electrophilic power of a molecule.

To expand the scope of cucurbituril and supramolecular chemistry, we have investigated its energetic and geometric properties with the means of DFT calculations. The DFT calculations were performed at the B3PW91/LANL2DZ level of theory.

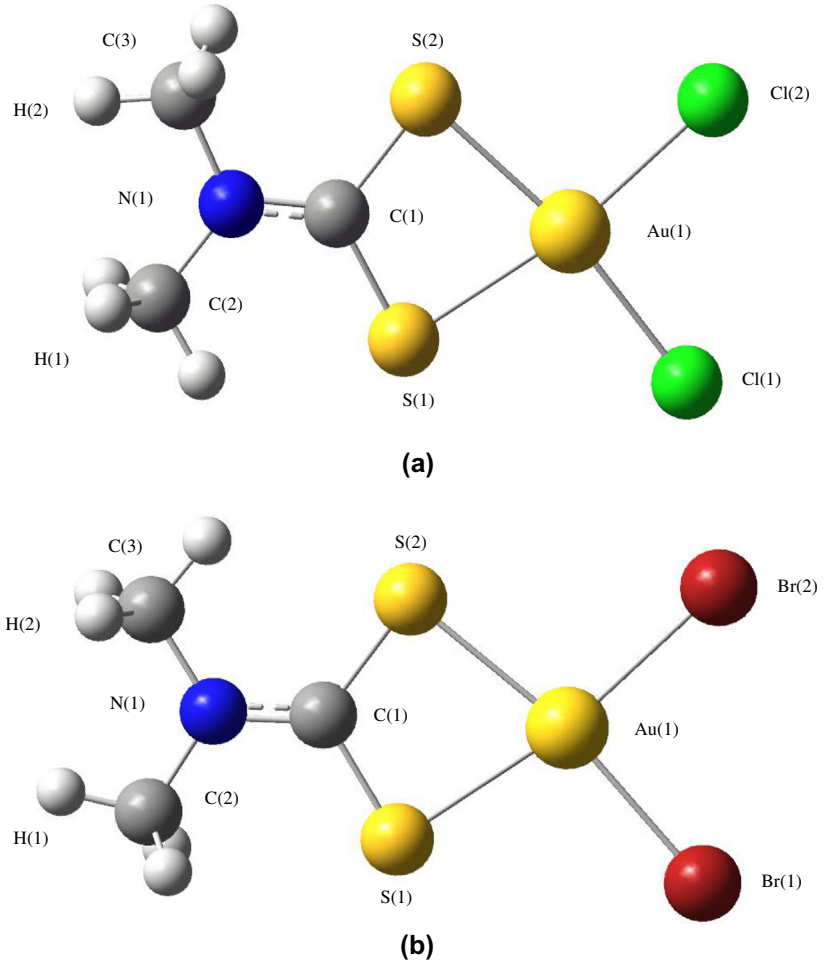

Figure 3 Optimized structures of (a) [DMDT(Au)Cl_2] and (b) [DMDT(Au)Br_2].

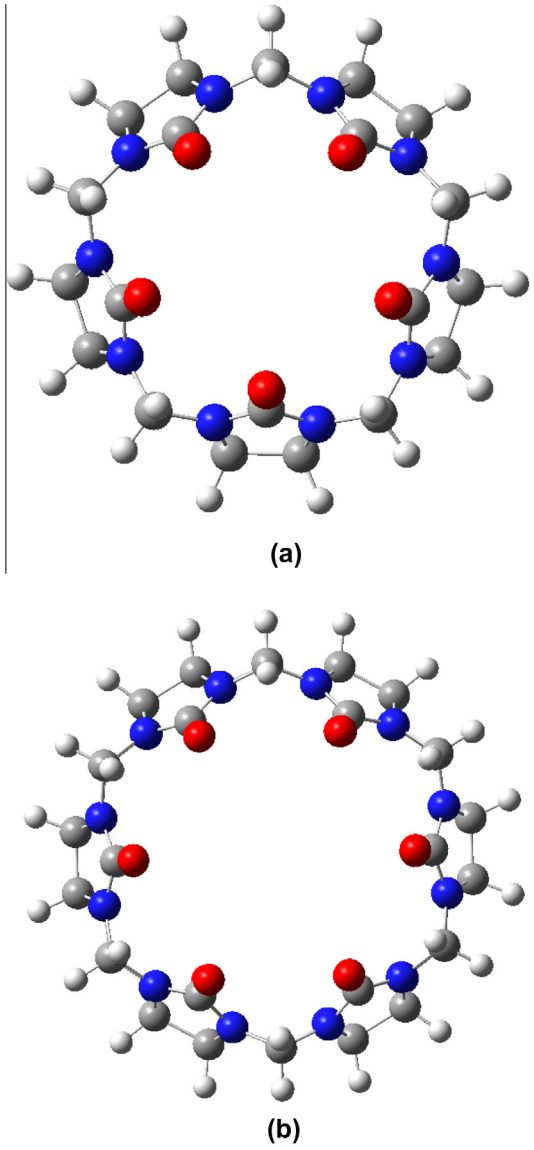

Figure 4 Final optimized structures of (a) CB[5] and (b) CB[6].

All the experimental and theoretical methods, when properly utilized in combination with each other, have proved to be extremely powerful in solving the structural, energetic, and dynamic problems associated with the CB[*n*] complexes.

In this research work, we have chosen Gold (III)-N,N-dimethyldithiocarbamate ([DMDT(Au)X_2] X = Cl, Br) complexes as anticancer molecules as shown in Fig. 1. The goal of the present study is to characterize, by accurate calculations, to predict the inclusion complex formation of gold(III) anticancer species with cucurbiturils (CB[*n* = 5,6]). We investigated the stabilization energy, heat of formation of the complexes, charge transfer, energies of the highest-occupied molecular orbital (HOMO) and lowest-unoccupied molecular orbital (LUMO) for the components and complexes as well as electronic properties and structural parameter i.e. bond lengths was calculated for the different complexes.

2. Computational method

Computational analysis of host–guest inclusion complex formation of the CB[*n* = 5, 6] with N,N-dimethyldithiocarbamate anticancer drugs was carried out, using the DFT calculation at the level of B3PW91/LANL2DZ, and employing the G03 package (Frisch et al., 2003). The initial geometries of anticancer drugs were optimized with DFT calculations using the Berny analytical gradient algorithm. Full geometry optimization of the CB[*n*] structures was performed without geometrical or symmetry restrains. Harmonic vibrational frequencies were computed for all structures. This allowed us to estimate the zero-point vibrational energy (ZPVE) correction for each structure, as well as to assess the nature of the stationary points and therefore to characterize whether they are true minima on the respective potential surfaces. The position of the guest molecules was determined by the *z* coordinates of the anticancer drugs. The $Z = 0$ point (center of the Cartesian coordinates) was chosen in the center of the CB[*n*] cavity. The inclusion process was simulated by placing the guest in one end of CB[*n*] cavity and then letting it pass through the CB[*n*] cavity by steps. In every step, single point calculations at the level of B3PW91/LANL2DZ were used to obtain the heat of formation of the host–guest complexes.

The electronic chemical potential (μ) was calculated as half of the energy of the Fermi level (E_{HOMO}) plus the first eigenvalue of the valence band (E_{LUMO}), as follows:

$$\mu = \frac{(E_{HOMO} + E_{LUMO})}{2} \tag{5}$$

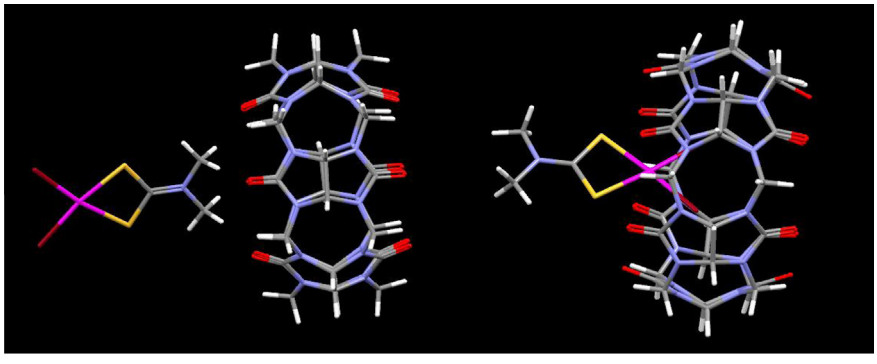

Figure 5 Geometrical structures of two orientations of penetration of [DMDT(Au)X_2] into the cavity of CB[*n*].

This definition was driven from Eq. (1). The operational definition of hardness (η) was obtained using a finite difference approximation to the second derivative in Eq. (2), as (Pearson, 1988):

$$\eta = \frac{(I - A)}{2} \tag{6}$$

where I and A are the ionization potential and the electron affinity of the system, respectively. Eq. (6) could be further approximated as follows, using Koopmans' theorem (Chattaraj and Poddar, 1999):

$$\eta = \frac{(E_{LUMO} - E_{HOMO})}{2} \tag{7}$$

Hard molecules thus have a large HOMO–LUMO gap and soft molecules have a small one (Pearson, 1988).

3. Result and discussion

All initial geometries of drugs and CB[n] were optimized in the framework of the density functional theory by use of the B3PW91 functional. The optimized geometries of cucurbit[n]uril n = 5–7, are consistent with the earlier experimental and modeling results (Bushchmann et al., 2006a, 2006b). Figs. 3 and 4 show that the final optimization geometries of [DMDT(Au)Cl_2], ([DMDT(Au)Br_2] and CB[n = 5,6].

The penetration of [DMDT(Au)X_2] in the cavity of the CB[n] can be done according to two orientations, A with the amine group of the drug and B with the halogen atoms of the drug (see Fig. 5). To determine the geometries of the possible CB[n]/[DMDT(Au)Cl_2] and CB[n]/[DMDT(Au)Br_2] complexes, [DMDT(Au)Cl_2] and ([DMDT(Au)Br_2] were placed in one end of the CB[n] cavity and then letting it pass through the CB[n] cavity which results indicate that the A orientation of [DMDT(Au)X_2] with CB[n] is significantly more favorable than that of B orientation.

The potential energy curve plots for the four different complexes of CB[5] and CB[6] with [DMDT(Au)Cl_2] and [DMDT(Au)Br_2] are shown in Fig. 6. Fig. 6 represents the penetration of anticancer drugs into the cavity of CB[n] with an amine group (A orientation). The structures of all complexes at the minimum energy were fully optimized using DFT calculations. The final geometry optimization of CB[n]/drugs show that the drugs were expelled from the cavity (Fig. 7).

To understand the stability of the complexes, the binding energy of CB[n]/[DMDT(Au)Cl_2] and CB[n]/[DMDT(Au)Br_2] complexes at the B3PW91 level of theory was calculated. The binding energy of complexes (ΔE) is obtained from the energy difference between the resulting complexes with the lowest HF (heat of formation) energy and the energy of the isolated cucurbit[n]urils and drugs as below:

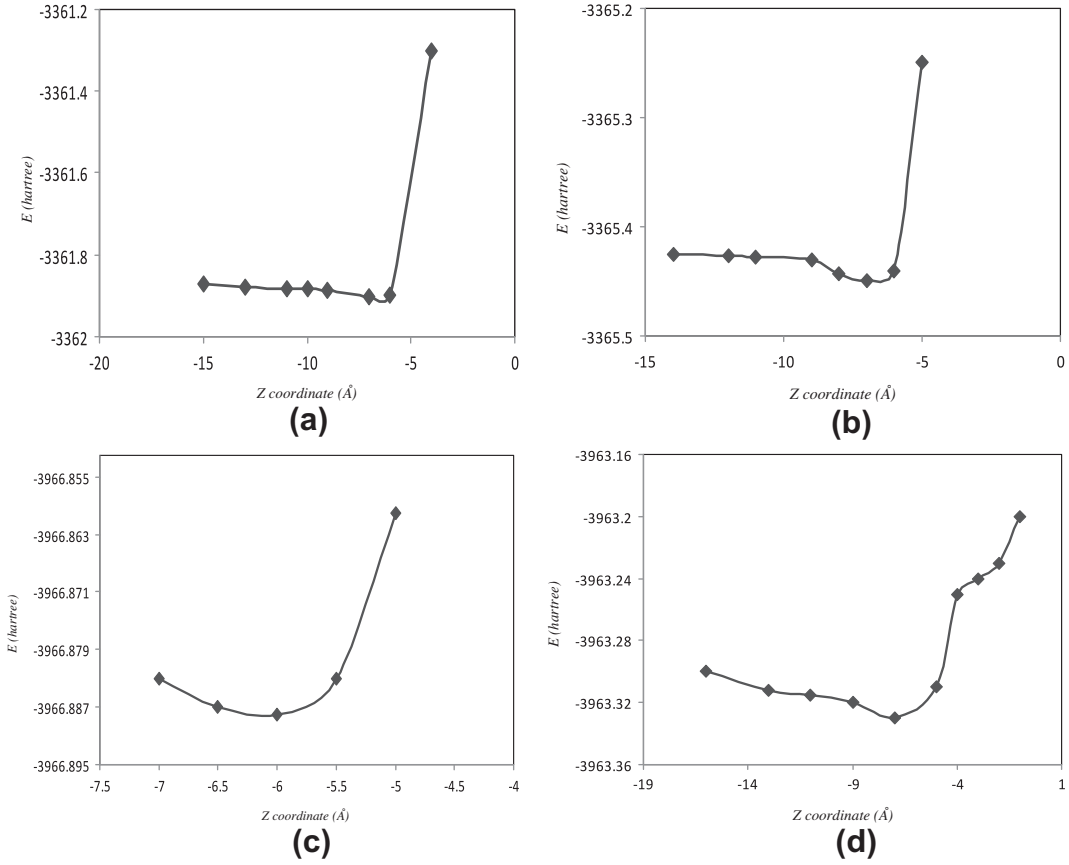

Figure 6 Graphic diagrams of A orientation for emulation of the inclusion complex formation of (a) CB[5]-[DMDT(Au)Br_2], (b) CB[5]-[DMDT(Au)Cl_2], (c) CB[6]-[DMDT(Au)Cl_2], (d) CB[6]-[DMDT(Au)Br_2] with DFT calculations. Position of the guest was determined by the Z-coordinate of the nitrogen atom in the alkyl amine group (the Z = 0 point was chosen in the center of the CB[n] cavity).

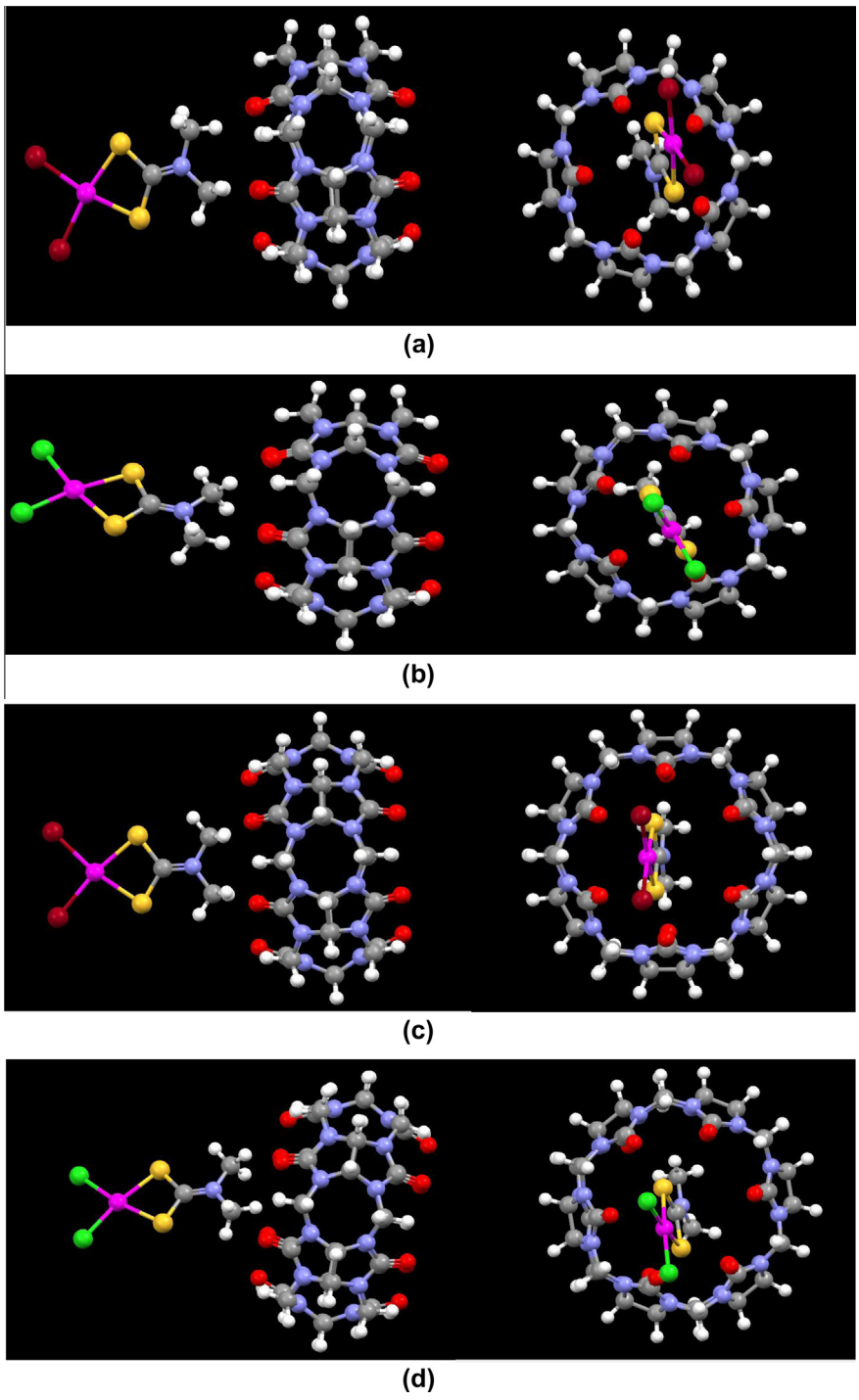

Figure 7 Optimized structures at each energy minimum obtained from DFT calculations for the bird's eye-view and the side view of (a) CB[5]-[DMDT(Au)Br_2], (b) CB[5]-[DMDT(Au)Cl_2], (c) CB[6]-[DMDT(Au)Br_2], (d) CB[6]-[DMDT(Au)Cl_2] complexes.

$$\Delta E = E_{complex} - (E_{CB[n]} + E_{drug}) \quad (8)$$

As can be seen in Table 1, the interaction between the cucurbit molecules and the drug molecules is quite strong: the binding energies of all complexes formed are about −87 kj/mol; which indicate that the inclusion complex process is exothermic and the complex formed is more stable. Negative interaction energies obtained from the DFT calculations show the complexation of the guests into the CB[*n*] cavities is highly favored. The effect of the cavity of CB[*n*] on the stability of the complexation was considered. The fit of the entire or at least a part of the guest molecule in the CB[*n*] host cavity determines the stability of the inclusion complex. The complexation energies reported in Table 1 have a negative value which means that the complexes formed are more stable than isolated species.

Table 1 Thermodynamic parameters upon the inclusion complexation of CB[n = 5, 6] with [DMDT(Au)Cl_2] and [DMDT(Au)Br_2] calculated by the DFT-based B3PW91/LANL2DZ method.

Compound	E_b (kj/mol)	ΔH(kj/mol)	ΔG(kj/mol)	ΔS(j/mol K)
[DMDT(Au)Cl_2]	–	–	–	–
[DMDT(Au)Br_2]	–	–	–	–
CB [5]	–	–	–	–
CB[6]	–	–	–	–
CB[5]/[DMDT(Au)Cl_2]	−86.788	−81.390	35.1397	−390.844
CB[5]/[DMDT(Au)Br_2]	−83.788	−78.214	32.827	−372.431
CB[6]/[DMDT(Au)Cl_2]	−88.327	−82.745	21.558	−349.834
CB[6]/[DMDT(Au)Br_2]	−90.269	−80.122	19.384	−333.746

E_{bind} *is* the binding energy of process.
ΔH is the enthalpy change of process.
ΔG is the Gibbs free energy change of process.
$\Delta S = (\Delta H - \Delta G)/T$ is the entropy change of the process.

Table 2 The significant bond lengths (Å) and the calculated NBO charges (esu) of optimized drugs and complexes of [(DMDT(Au)Cl_2] with CB[n = 5,6]urils calculated by the B3PW91/LANL2DZ method.

	[(DMDT(Au)Cl_2]	[(DMDT(Au)Cl_2]/CB[5]	[(DMDT(Au)Cl_2]/CB[6]
Bond lengths (Å)			
Au(1)–Cl(1)	2.398	2.412	2.412
Au(1)–Cl(2)	2.398	2.412	2.415
Au(1)–S(1)	2.466	2.454	2.453
Au(1)–S(2)	2.467	2.454	2.452
N(1)–C(1)	1.332	1.317	1.316
N(1)–C(2)	1.475	1.480	1.479
N(1)–C(3)	1.478	1.482	1.483
C(1)–S(1)	1.789	1.799	1.800
C(1)–S(2)	1.789	1.800	1.799
C(2)–H(1)	1.091	1.094	1.093
C(3)–H(4)	1.092	1.093	1.093
Charge (esu)			
Au(1)	0.32435	0.84762	0.82727
S(1)	0.07597	−0.05436	−0.05196
S(2)	0.08257	−0.05978	−0.03627
Cl(1)	−0.29990	−0.47456	−0.48625
Cl(2)	−0.29993	−0.47538	−0.48470
N(1)	−0.41526	−0.39265	−0.38981
C(1)	−0.04923	−0.03635	−0.03213
C(2)	−0.42344	−0.43104	−0.42812
C(3)	−0.43665	−0.43330	−0.43691
H(1)	0.24297	0.22959	0.22480
H(2)	0.23662	0.26516	0.26000
H(3)	0.23690	0.26389	0.26559
H(4)	0.24250	0.23590	0.25042
H(5)	0.24467	0.22712	0.25642
H(6)	0.23786	0.27384	0.25069

The value of binding energy for CB[5]/[DMDT(Au)Cl_2] and CB[5]/[DMDT(Au)Br_2] complexes (about −85.0 kj/mol) in the inclusion process indicates that the cavity of CB[5] is good for acceptance of the drugs as guest molecule in the cavity itself. The key features in the complexation are summarized in Table 1. With the change in the host molecule from CB[5] to CB[6], the stability of the formed complexes is slightly increased. In other words, the complex formed between CB[6] and drugs is more stable than CB[5]/drugs. As a result, with the increase in the size of the cavities of the CB[n], the stability of the formed complexes is increased. Obtained data are in agreement with the results of the inclusion complex formation between CB[n] and oxaliplatin (Suvitha et al., 2010). Venkataramanan et al. used a theoretical method based on first principles which show that the formation energy increases with the increase in the size of CB[n]. To investigate the thermodynamic parameters of the inclusion processes the statistical thermodynamic calculations were carried out at 1 atm and 298.15 K

Table 3 The significant bond lengths (Å) and the calculated NBO charges (esu) of optimized drugs and complexes of [(DMDT(Au)Br_2] with CB[n = 5,6]urils calculated by the B3PW91/LANL2DZ method.

	[(DMDT(Au)Br_2]	[(DMDT(Au)Br_2]/CB[5]	[(DMDT(Au)Br_2]/CB[6]
Bond lengths (Å)			
Au(1)–Br(1)	2.535	2.549	2.552
Au(1)–Br(2)	2.536	2.548	2.551
Au(1)–S(1)	2.483	2.469	2.465
Au(1)–S(2)	2.484	2.470	2.465
N(1)–C(1)	1.333	1.318	1.318
N(1)–C(2)	1.474	1.480	1.481
N(1)–C(3)	1.478	1.482	1.481
C(1)–S(1)	1.787	1.798	1.802
C(1)–S(2)	1.788	1.798	1.802
C(2)–H(1)	1.091	1.094	1.093
C(3)–H(4)	1.092	1.095	1.092
Charge (esu)			
Au(1)	0.18055	0.16178	0.16255
S(1)	0.06489	0.06432	0.06176
S(2)	0.07046	0.05681	0.06170
Br(1)	−0.21383	−0.26236	−0.27397
Br(2)	−0.21216	−0.26251	−0.27396
N(1)	−0.41707	−0.38654	−0.38544
C(1)	−0.04941	−0.02156	−0.01627
C(2)	−0.42377	−0.43209	−0.42917
C(3)	−0.43738	−0.43491	−0.42926
H(1)	0.24327	0.22971	0.23075
H(2)	0.23558	0.27053	0.25951
H(3)	0.23560	0.26278	0.26252
H(4)	0.24321	0.23328	0.23083
H(5)	0.24335	0.22888	0.26251
H(6)	0.23671	0.27713	0.25961

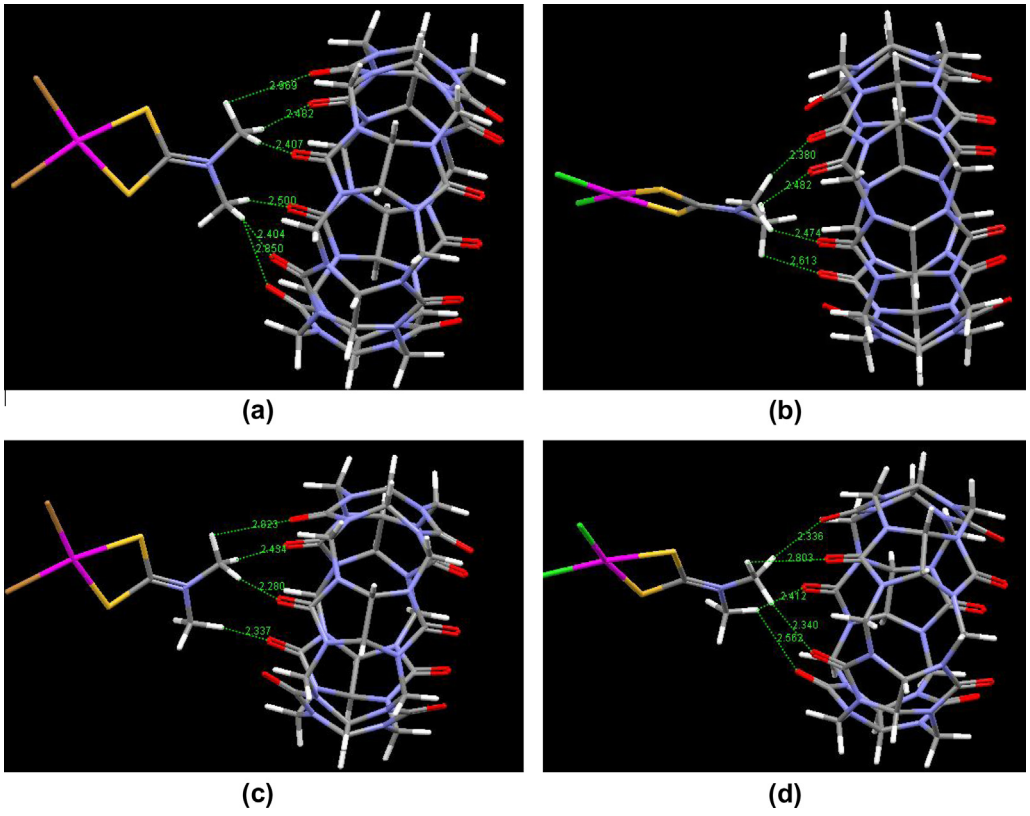

Figure 8 The nearest intermolecular distances between hydrogen atom of drug with oxygen atom of CB[n]; (a) CB[6]/[DMDT(Au)Br_2], (b) CB[6]/[DMDT(Au)Cl_2], (c) CB[5]/[DMDT(Au)Br_2], (d) CB[5]/[DMDT(Au)Cl_2].

Table 4 HOMO, LUMO and Gap energy, chemical potential (μ), hardness (η) and electrophilicity (ω) of the drugs, CB[*n*]s and inclusion complexes CB[*n*]/drugs.

Compound	HOMO (eV)	LUMO (eV)	Gap (eV)	μ (eV)	η (eV)	ω
$DMDT(Au)Cl_2$	−7.458	−4.658	2.780	−6.058	1.400	13.108
$DMDT(Au)Br_2$	−6.951	−4.592	2.360	−5.772	1.1796	14.118
CB[5]	−6.657	0.389	7.046	−3.134	3.523	1.394
CB[6]	−6.230	1.123	7.354	−2.554	3.677	0.887
CB[5]/$DMDT(Au)Cl_2$	−6.278	−3.353	2.925	−4.815	1.463	7.927
CB[5]/$DMDT(Au)Br_2$	−6.096	−3.625	2.471	−4.860	1.235	9.562
CB[6]/$DMDT(Au)Cl_2$	−6.4189	−3.489	2.930	−4.954	1.465	8.374
CB[6]/$DMDT(Au)Br_2$	−5.930	−3.419	2.510	−4.675	1.255	8.705

using B3WP91/LANL2DZ. The thermodynamic parameters such as the Gibbs free energy changes (ΔG), the enthalpy changes (ΔH), and the entropy changes of the process (ΔS) were calculated. The results, summarized in Table 1, show that the values of Gibbs free energy changes (ΔG) for all structures are positive, which imply that they do not occur spontaneously at room temperature. On the other hand, the obtained values for enthalpy changes (ΔH) for all complexes are negative, which means that the processes are exothermic.

We now turn to a discussion of the structural parameters of their complexes. The structural parameters calculated by the B3PW91 method of the isolated CB[5] and CB[6] and of their complexes with [$DMDT(Au)Cl_2$] and [$DMDT(Au)Br_2$] are presented in Tables 2 and 3. These results indicate that there are no significant changes in bond lengths; this is mainly observed for the bonding involving the nitrogen atom during the inclusion processes. The nearest intermolecular distance between CB[*n*] and drugs to investigate the hydrogen bonds was considered. The final optimization structures of complexes (Fig. 8) show that the nearest distance was found between the oxygen atom of carbonyl portal groups of CB[*n*] and H atoms of amine group of drugs. In these cases, the anticancer drugs are embedded in the CB[*n*] cavity, which is consistent with the structures suggested by NMR spectroscopy (Oh et al., 2001). The amine nitrogen atom of drug essentially lie on the plane made by five and six oxygen atoms of CB[5] and CB[6] portal while forming hydrogen bonds with the oxygen atom. From Fig. 8, we find that the six oxygen atoms of CB[6] form strong interactions with five hydrogen (C═O–H = 2.607 Å) and the nearest distance between H atom of [$DMDT(Au)Br_2$] and O atom of CB[6] in CB[6]/[$DMDT(Au)Br_2$] complex is obtained as about 2.602 Å. Also, the hydrogen intermolecular interactions for CB[6]/[$DMDT(Au)Cl_2$] complex are considered. When the guest molecule changed from [$DMDT(Au)Br_2$] to [$DMDT(Au)Cl_2$], the average intermolecular distance changed to 2.487 Å (C═O–H = 2.487 Å). In addition, four hydrogen bonds were found for the CB[6]/[$DMDT(Au)Cl_2$] complex from Fig. 8, which means that the CB[6]/[$DMDT(Au)Br_2$] complex is slightly more stable than CB[6]/[$DMDT(Au)Cl_2$]. These results are in well agreement with the results of the stabilization energy. As a result, the synergetic effects of the hydrogen bonding appear to be the major factor for the stability of the complexes.

If the host molecule from CB[6] changed to CB[5], the nearest intermolecular distances and the numbers of hydrogen bonding changed. For the CB[5]/[$DMDT(Au)Cl_2$] complex, five glycol-uril carbonyl groups form five hydrogen bonding with five hydrogen atoms of [$DMDT(Au)Cl_2$] with the nearest

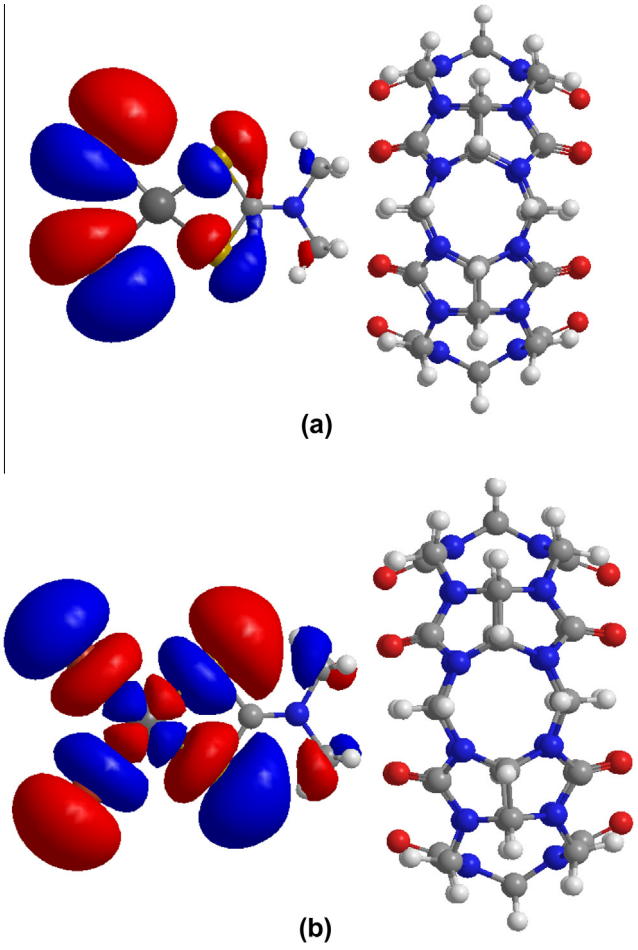

Figure 9 Typical counter plots of (a) HOMO and (b) LUMO for the A orientations of the CB[6]-[$DMDT(Au)Br_2$] complex.

intermolecular distance about 2.491 Å while the CB[5]/[$DMDT(Au)Br_2$] complex forms just four hydrogen bonding with (C═O–H = 2.469 Å) which means that the CB[5]/[$DMDT(Au)Cl_2$] complex is slightly more stable than CB[5]/[$DMDT(Au)Br_2$] (see Fig. 8).

One of the essential characteristics affecting the possibility of interaction of the host–guest complexes inside the cavity is the distribution of effective charges on the atoms. Tables 2 and 3 indicate that the partial charge of the Au, Cl, Br, N and H atoms of drugs significantly changed during the complexation. Charge distribution computed by the natural bond

orbital (NBO) approach reveals that the charges of the Cl(1), Cl(2), Br(1) and Br(2) atoms of [DMDT(Au)Br_2] and [DMDT(Au)Cl_2] in the complexes are more negative than those in the isolated components while the H atoms are more positive than those in the isolated drugs. This means that when the guest molecule interacts with CB[*n*], its charge distribution changes. So, when [DMDT(Au)Br_2] and [DMDT(Au)Cl_2] molecules penetrate into the CB[*n*] cavities by alkyl groups, there is a charge-transfer from drugs to CB[*n*] producing a common chemical potential so, that strong hydrogen bonding occur. The atomic numbering schemes of drugs are shown in Fig. 3.

The results of the HOMO and LUMO energies of the complexes are summarized in Table 4. The most important terms in this kind of interaction are contributed from the partial charge transfer between the HOMO of one component and the LUMO of another. The HOMO–LUMO (H–L) energy gap for these complexes is 2.5–3.0 eV. According to the difference between the frontier orbital energies when the energy gap is higher, the system behaves like a very stable molecule. In addition, the high HOMO energy indicates that the molecule can undergo an electrophilic attack with a large probability. These results indicate that the HOMO orbital is localized on the drugs and the LUMO orbital is observed on the CB[*n*]. The typical counter plots of HOMO and LUMO of CB[6]/[DMMT(Au)Br_2 are shown in Fig. 9.

The global indices of reactivity in the context of DFT are presented in Table 4. The value of electronic chemical potential, hardness and electrophilicity for complexes are differing from the individual CB[*n*] and drug molecules. When drug molecule and CB[*n*] are brought together, electrons will flow from lower electronegativity (χ) to that of higher χ. On the other hand, electrons are transferred to the lower electronic chemical potential, until the electronic chemical potentials become equal (Pearson, 1988). The difference in electronegativity drives the electron transfer, and the sum of the hardness parameters acts as a resistance. As a result, the electrons will flow from a definite occupied orbital in drugs and will go into a definite empty orbital in CB[*n*]. Also, results indicate that when the drug molecules penetrate into the cavity of the CB[n], the hardness of the complexes decreased, which means that the stability of the complexes is lower than pristine CB[*n*].

4. Conclusion

The purpose of this research work is an attempt to explain the inclusion complex formation of [DMDT(Au)Cl_2] and [DMDT(Au)Br_2] with cucurbit [n = 5, 6] urils using DFT calculation. We took into account only the stoichiometry 1:1. To summarize, the following conclusion can be made. Molecular modeling calculations, predict that [DMDT(Au)X_2] was expelled from the cavity of CB[n = 5,6]. The analyses of the thermodynamic calculations indicate that the enthalpy contribution is favorable to the complex formation. Results of the binding energy show that the CB[6]/[DMDT(Au)Br_2] complex is more stable than others. The final optimization geometries show that the hydrogen bonding between the portal oxygen atom of CB[*n*] and the hydrogen atom of amine group of drugs and electrostatic interactions are the major factors contributing to the overall stabilities of the complexations.

References

Alama1, A., Tasso, B., Novelli, F., Sparatore, F., 2009. Organometallic compounds in oncology: implications of novel organotins as antitumor agent. Drug Discov. Today 14, 500–508.

Anconi, C.P.A., Silva Delgado, L.D., Dos Reis, J.B.A., De Almeida, W.B., Costa, L.A.S., Dos Santos, H.F., 2011. Inclusion complexes of alpha-cyclodextrin and the cisplatin analogues oxaliplatin, carboplatin and nedaplatin: a theoretical approach. Chem. Phys. Lett. 515, 127–131.

Bakovets, V.V., Masliy, A.N., Kuznetsov, A.M., 2008. Formation thermodynamics of cucurbit[6]uril macrocycle molecules: a theory study. J. Phys. Chem. B 112, 12010–12013.

Bali, M.S., Buck, D.P., Coe, A.J., Day, A.I., Collins, J.G., 2006. Cucurbituril binding of trans-[{PtCl(NH_3)(2)}(2)(mu-NH_2(CH_2)(8)NH_2)](2+) and the effect on the reaction with cysteine. Dalton Trans., 5337–5344.

Behrend, R., Meyer, E., Rusche, F., 1905. Ueber condensationsproducte aus glycoluril und formaldehyd. Liebigs Ann. Chem. 339, 1–37.

Buschmann, H.J., Wego, A., Zielesny, A., Schollmeyer, E., 2006a. Structure, electronic properties and NMR-shielding of cucurbit[n]urils. J. Incl. Phenom. Macrocycl. Chem. 54, 85–88.

Bushchmann, H.J., Wego, A., Zielesny, A., Schollmeyer, E., 2006b. Structure, stability, electronic properties and NMR-shielding of the cucurbit[6]uril–spermine-complex. J. Incl. Phenom. Macrocycl. Chem. 54, 241–246.

Chattaraj, P.K., Poddar, A., 1999. Molecular reactivity in the ground and excited electronic states through density-dependent local and global reactivity parameters. J. Phys. Chem. A 103, 8691–8699.

Faustino, C.M.C., Calado, A.R.T., Garcia-Rio, L., 2011. Mixed micelle formation between amino acid-based surfactants and phospholipids. J. Colloid Interface Sci. 359, 493–498.

Freeman, W.A., Mock, W.L., Shih, N.Y., 1981. Cucurbituril. J. Am. Chem. Soc. 103, 7367–7368.

Frisch, M.J., et al. 2003. Gaussian, Inc., Pittsburgh, PA.

Gabbiani, C., Casini, A., Messori, L., 2007. Gold(III) compounds as anticancer drugs. Gold Bull. 40, 73–81.

Giovagnini, L., Ronconi, L., Aldinucci, D., Lorenzon, D., Sitran, S., Fregona, D., 2005. Synthesis, characterization, and comparative in vitro cytotoxicity studies of platinum(II), palladium(II), and gold(III) methylsarcosine dithiocarbamate complexes. J. Med. Chem. 48, 1588–1595.

Jeon, Y.J., Kim, S.Y., Ko, Y.H., Sakamoto, S., Yamaguchi, K., Kim, K., 2005. Novel molecular drug carrier: encapsulation of oxaliplatin in cucurbit[7]uril and its effects on stability and reactivity of the drug. Org. Biomol. Chem. 3, 2122–2125.

Kelland, L., 2007. The resurgence of platinum-based cancer chemotherapy. Nature 7, 573–584.

Kim, J., Jung, I., Kim, S., Lee, S.Y., Kang, E.J.K., Sakamoto, S., Yamaguchi, K., Kim, K., 2000. New cucurbituril homologues: syntheses, isolation, characterization, and X-ray crystal structures of cucurbit[n]uril (n = 5, 7, and 8). J. Am. Chem. Soc. 122, 540–541.

Lagona, J., Mukhopadhyay, P., Chakrabarti, S., Isaacs, L., 2005. The Cucurbit[n]uril family. Angew. Chem. Int. Ed. 44, 4844–4870.

Lei, W., Jiang, G., Zhou, Q., Zhang, B., Wang, X., 2010. Greatly enhanced binding of a cationic porphyrin towards bovine serum albumin by cucurbit[8]uril. Phys. Chem. Chem. Phys. 12, 13255–13260.

Liu, S., Zavalij, P.Y., Isaacs, L., 2005. Cucurbit[10]uril. J. Am. Chem. Soc. 127, 16798–16799.

Louie, A.Y., Meade, T.J., 1999. Metal complexes as enzyme inhibitors. Chem. Rev. 99, 2711–2734.

Marquez, C., Hudgins, R.R., Nau, W.M., 2004. Mechanism of host-guest complexation by cucurbituril. J. Am. Chem. Soc. 126, 5806–5816.

Marzano, C., Ronconi, L., Chiara, F., Giron, M.C., Faustinelli, I., Cristofori, P., Trevisan, A., Fregona, D., 2011. Gold(III)-dithiocarbamato anticancer agents: activity, toxicology and histopathological studies in rodents. Int. J. Cancer 129, 487–496.

Oh, K.S., Yoon, J., Kim, K.S., 2001. Structural stabilities and self-assembly of cucurbit[n]uril (n = 4–7) and decamethylcucurbit[n]uril (n = 4–6): a theoretical study. J. Phys. Chem. B 105, 9726–9731.

Ott, I., 2009. On the medicinal chemistry of gold complexes as anticancer drugs. Coordination Chem. Rev. 253, 1670–1681.

Parr, R.G., Pearson, R.G., 1983. Absolute hardness: companion parameter to absolute electronegativity. J. Am. Chem Soc. 105, 7512–7516.

Parr, R.G., Yang, W., 1984. Density functional approach to the frontier-electron theory of chemical reactivity. J. Am. Chem. Soc. 106, 4049–4050.

Parr, R.G., Yang, W., 1989. Density Functional Theory of Atoms and Molecules. Oxford University Press, New York.

Pearson, R.G., 1973. Hard and Soft Acid and Bases. Dowden, Hutchinson and Ross, Stroudsburg, PA.

Pearson, R.G., 1987. Recent advances in the concept of hard and soft acids and bases. J. Chem. Edu. 64, 561–567.

Pearson, R.G., 1988. Absolute electronegativity and hardness: application to inorganic chemistry. Inorg. Chem. 27, 734–740.

Pearson, R.G., 1993. The principle of maximum hardness. Acc. Chem. Res. 26, 250–255.

Pearson, R.G., 1997. Chemical Hardness: Applications from Molecules to Solids. Wiley-VCH Verlag GMBH, Weinheim Germany.

Pearson, R.G., Donnelly, R.A., Levy, M., Palke, W.E., 1978. Electronegativity: the density functional viewpoint. J. Chem. Phys. 68, 3801–3807.

Pearson, R.G., Szentpaly, L., Liu, S., 1999. Electrophilicity index. J. Am. Chem. Soc. 121, 1922–1924.

Pichierri, F., 2006. DFT study of cucurbit[n]uril, n = 5-10. 2006. J. Mol. Struct. (Theochem.) 765, 151–152.

Pinjari, R.V., Gejji, S.P., 2008. Electronic structure, molecular electrostatic potential, and NMR chemical shifts in cucurbit[n]urils (n = 5-8), ferrocene, and their complexes. J. Phys. Chem. A 112, 12679–12686.

Robertson, J.D., Orrenius, S., 2002. Role of mitochondria in toxic cell death. Toxicology 181, 491–496.

Ronconi, L., Giovagnini, L., Marzano, C., Bettio, F., Graziani, R., Pilloni, G., Fregona, D., 2005. Gold dithiocarbamate derivatives as potential antineoplastic agents: design, spectroscopic properties, and in vitro antitumor activity. Inorg. Chem. 44, 1867–1881.

Ronconi, L., Marzano, C., Zanello, P., Corsini, M., Miolo, G., Macca, C., Trevisan, A., Fregona, D., 2006. Gold(III) dithiocarbamate derivatives for the treatment of cancer: solution chemistry, DNA binding, and hemolytic properties. J. Med. Chem. 49, 1648–1657.

Sancho, M.I., Gasull, E., Blanco, S.E., Castro, E.A., 2011. Inclusion complex of 2-chlorobenzophenone with cyclomaltoheptaose (beta-cyclodextrin): temperature, solvent effects and molecular modeling. Carbohydr. Res. 346, 1978–1984.

Sen, K.D., Jorgensen, C.K., 1987. Electronegativity, Structure and Bonding. Springer-Verlag, New York.

Suvitha, A., Venkataramanan, N.S., Mizuseki, H., Kawazoe, Y., Ohuchi, N., 2010. Theoretical insights into the formation, structure, and electronic properties of anticancer oxaliplatin drug and cucurbit[n]urils n = 5 to 8. J. Incl. Phenom. Macrocycl. Chem. 66, 213–218.

Wang, R., Macartney, D.H., 2008. Cucurbit[7]uril stabilization of a diarylmethane carbocation in aqueous solution. Tetrahedron Lett. 49, 311–314.

Wheate, N.J., 2008. Improving platinum(II)-based anticancer drug delivery using cucurbit[n]urils. J. Inorg. Biochem. 102, 2060–2066.

Wheate, N.J., Day, A.I., Blanch, R.J., Arnold, A.P., Cullinane, C., Collins, J.G., 2004. Multi-nuclear platinum complexes encapsulated in cucurbit[n]uril as an approach to reduce toxicity in cancer treatment. Chem. Commun. 12, 1424–1425.

Wyman, I.W., Macartney, D.H., 2010. Host-guest complexations of local anaesthetics by cucurbit[7]uril in aqueous solution. Org. Biomol. Chem. 8, 247–252.

Yang, W., Parr, R.G., 1985. Hardness, softness, and the fukui function in the electronic theory of metals and catalysis. Proc. Natl. Acad. Sci. USA 82, 6723–6726.